



Cite this: *Chem. Sci.*, 2022, **13**, 10904

All publication charges for this article have been paid for by the Royal Society of Chemistry

## A versatile *o*-aminoanilide linker for native chemical ligation†

Iván Sánchez-Campillo, <sup>a</sup> Judit Miguel-Gracia, <sup>a</sup> Periklis Karamanis <sup>‡,b</sup> and Juan B. Blanco-Canosa <sup>\*a</sup>

Chemical protein synthesis (CPS) is a consolidated field founded on the high chemospecificity of amide-forming reactions, most notably the native chemical ligation (NCL), but also on new technologies such as the Ser/Thr ligation of C-terminal salicylaldehyde esters and the  $\alpha$ -ketoacid-hydroxylamine (KAHA) condensation. NCL was conceptually devised for the ligation of peptides having a C-terminal thioester and an N-terminal cysteine. The synthesis of C-terminal peptide thioesters has attracted a lot of interest, resulting in the invention of a wide diversity of different methods for their preparation. The *N*-acylurea (Nbz) approach relies on the use of the 3,4-diaminobenzoic (Dbz-COOH) and the 3-amino-(4-methylamino)benzoic (MeDbz-COOH) acids; the latter disclosed to eliminate the formation of branching peptides. Dbz-COOH has been also used for the development of the benzotriazole (Bt)-mediated NCL, in which the peptide-Dbz-CONH<sub>2</sub> precursor is oxidized to a highly acylating peptide-Bt-CONH<sub>2</sub> species. Here, we have brought together the Nbz and Bt approaches in a versatile linker, the 1,2-diaminobenzene (Dbz). The Dbz combines the robustness of MeDbz-COOH and the flexibility of Dbz-COOH: it can be converted into the Nbz or Bt C-terminal peptides. Both are ligated in high yields, and the reaction intermediates can be conveniently characterized. Our results show that the Bt precursors have faster NCL kinetics that is reflected by a rapid transthioesterification (<5 min). Taking advantage of this major acylating capacity, peptide-Bt can be transselenoesterified in the presence of selenols to afford peptide selenoesters which hold enormous potential in NCL.

Received 25th July 2022  
Accepted 25th August 2022

DOI: 10.1039/d2sc04158h  
[rsc.li/chemical-science](http://rsc.li/chemical-science)

## Introduction

Native chemical ligation (NCL) forms with exclusive selectivity an amide bond between a C-terminal peptide  $\alpha$ -thioester (peptide-COSR) and an N-terminal cysteinyl-peptide (Cys-peptide) under reaction conditions resembling the physiological ones.<sup>1,2</sup> The chemospecific nature of this reaction prevents the need for the side chain protection of peptides, and thus it can be used just as effectively in recombinant protein-COSR obtained by splicing of protein-intein fusions.<sup>3</sup> Further elaborations of the NCL extended the reaction to other N-terminal residues,<sup>4–7</sup> peptide selenoesters<sup>8</sup> and selenoester-diselenide ligations.<sup>9</sup> Since Fmoc-solid phase peptide synthesis (Fmoc-SPPS) is currently the most adopted methodology for peptide synthesis, the direct preparation of peptide thioesters is poorly efficient, necessitating other approaches that overcome the

piperidine-mediated aminolysis of the peptide-COSR. Some of these methods include the Kenner's sulfonamide,<sup>10,11</sup> pyroglutamyl imides,<sup>12</sup> cyclic urethane at Ser side chain-backbone sites,<sup>13</sup> acyl hydrazides,<sup>14</sup> SEALide<sup>15</sup> and other intramolecular *O* or *N*-to-*S* acyl scaffolds,<sup>16–19</sup> benzotriazoles (Bt)<sup>20,21</sup> and the *N*-acylurea (Nbz).<sup>22–24</sup> These approaches rely on the use of thioester precursors (also called crypto-thioesters) that, upon activation under specific conditions, can be trapped in the presence of thiols that form the active peptide-COSR. For instance, the SEALide is masked off through an intramolecular disulfide bond, and the addition of TCEP initiates the reduction of the disulfide bridge that allows the *N*-to-*S* acyl shift and subsequent transthioesterification.<sup>15</sup> On the other hand, acyl hydrazides are popular due to their straightforward synthesis and activation, either by nitrite oxidation to yield acyl azides<sup>14</sup> or acetyl acetone condensation to afford acyl pyrazoles.<sup>25</sup>

The Nbz method has been also used for the chemical synthesis of a broad range of proteins. Disclosed in 2008,<sup>22</sup> it is based on the 3,4-diaminobenzoic (Dbz-COOH) scaffold (Scheme 1). Monoacylation of the Dbz-CONH-resin, preferentially at the *m*-amine, followed by stepwise chain elongation, results in a peptide1-Dbz-CONH-resin (**1a**). Then, the free amine of the *o*-aminoanilide **1a** is acylated with *p*-nitrophenyl chloroformate, and the resulting 3-peptidyl-4-(*p*NO<sub>2</sub>)

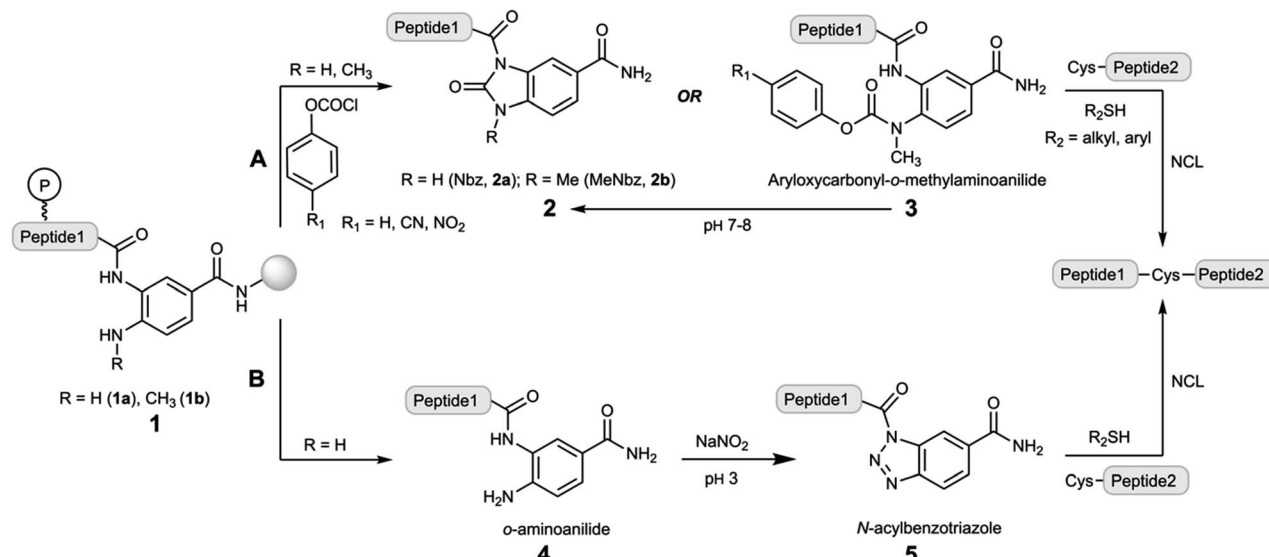
<sup>a</sup>Institute for Advanced Chemistry of Catalonia (IQAC-CSIC), Jordi Girona 18-26, 08034 Barcelona, Spain. E-mail: [juanbautista.blanco@iqac.csic.es](mailto:juanbautista.blanco@iqac.csic.es)

<sup>b</sup>Dept. of Chemistry "G. Ciamician", University of Bologna, Via Selmi 2, 40126, Bologna, Italy

† Electronic supplementary information (ESI) available. See <https://doi.org/10.1039/d2sc04158h>

‡ Present address: School of Chemistry, University College Dublin (UCD), Belfield, Dublin 4, D04 N2E2, Ireland.





**Scheme 1** Previous work: synthetic avenues of 1,2-diaminobenzyl derivatives for chemical protein synthesis. Following the route A, the peptide1–Dbz/MeDbz–CONH–resin is converted in the peptide1–Nbz/MeNbz–CONH<sub>2</sub> on resin or in solution through a phosgenation-type process. Next, this peptide is ligated through NCL to another Cys-peptide2. In the route B, the peptide1–Dbz–CONH<sub>2</sub> is transformed in peptide1–Bt–CONH<sub>2</sub> and then ligated to a Cys-peptide2. P = protecting group.

phenyloxycarbonyl)Dbz–CONH–resin undergoes intramolecular cyclization under basic conditions to yield the peptide1–Nbz–CONH–resin product (Scheme 1 route A). After TFA-mediated acidolytic cleavage, the unprotected peptide1–Nbz–CONH<sub>2</sub> (**2a**) is obtained in solution. This acyl-Nbz–CONH<sub>2</sub> activated peptide **2a** can react with Cys-peptide2 at neutral pH, although the slow ligation rates rather reduce the synthetic applicability of the direct condensation due to a faster hydrolysis. However, in the presence of exogenous thiols, the rapid thioesterification of **2a** streamlines the NCL in high conversions (>95%).<sup>22</sup>

It is worth mentioning that during the Fmoc-SPPS, the *o*-aminoanilide of **1a** remains mostly unmodified although unprotected. However, under specific conditions, *i.e.* microwave-assisted Fmoc-SPPS, use of basic coupling protocols and, especially, fragments containing Gly-rich sequences, the *o*-aminoanilide is acylated precluding further conversion to **2a**.<sup>23,26</sup> Therefore, apart from considering other strategies that involve the orthogonal protection of the *o*-aminoanilide,<sup>26,27</sup> the methylation of the *p*-amino group provided a new linker, 3-amino-4-(methyl)aminobenzoic acid (MeNbz–COOH), that overcame the overacylation while it still undergoes MeNbz formation on resin<sup>23</sup> (**2b**) or in aqueous solution (**3**, Scheme 1 route A).<sup>24</sup> Several proteins have been synthesized using the Nbz/MeNbz methodology including ubiquitin chains,<sup>28</sup> cyclotides,<sup>29</sup>  $\alpha$ -synuclein,<sup>30</sup> the human selenoproteins SELW<sup>31</sup> and F,<sup>32</sup> and the transactivation domain of p53.<sup>33</sup>

In addition, the *o*-aminoanilide peptide1–Dbz–CONH<sub>2</sub> (**4**) can undergo a chemoselective oxidation by sodium nitrite at acidic pH to give a peptide1–Bt–CONH<sub>2</sub> (**5**) species, that is highly acylating and can be also intercepted by thiols to form a peptide–COSR (Scheme 1 route B).<sup>20,21,34</sup> Although this route B has not received similar attention as for route A, the synthetic

potential has been underestimated, particularly its use in sequential NCL.<sup>35</sup>

Besides CPS, the Nbz/MeNbz and Bt linkers have found other important applications, enabling the access to posttranslational modifications at the C-terminal peptide side of high structural and biomedical relevance, including C-terminal peptide esters and *N*-alkylamides and<sup>36–38</sup> head-to-tail and side chain-to-tail cyclic peptides.<sup>39–41</sup>

From a synthetic point of view, it would be very attractive to use a single 1,2-diaminobenzene-type moiety for the preparation of peptides featuring C-terminal Nbz and Bt-type functionalities that combines the advantages of Dbz–COOH and MeDbz–COOH. Here, we show that C-terminal peptides amidated with 1,2-diaminobenzene (Dbz) can be efficiently converted in peptide–Nbz or peptide–Bt derivatives from the same initial peptide–Dbz–PAL–resin (PAL = 4-(aminomethyl)-3,5-dimethoxyphenoxy)butanoic/pentanoic acid) precursor.

## Results and discussion

### Fmoc-SPPS of peptide–Dbz–PAL

Despite the Dbz–COOH compatibility with the Nbz and Bt approaches, the undesired side-acylations of the *o*-aminoanilide required the use of orthogonal protection for the *p*-amino group.<sup>26,27</sup> Nevertheless, a facile and straightforward strategy based on a robust *o*-aminoanilide derivative would increase the final yield and purity. Thus, the Dbz group has been previously incorporated into different TFA-labile handles including Wang,<sup>42</sup> 2-Cl-trityl<sup>43</sup> and Rink,<sup>43</sup> to synthesize peptide–Bt derivatives. Unfortunately, when the synthesis was carried out, the steric hindrance led to incomplete acylations with *p*-nitrophenyl chloroformate in the peptide–Dbz–2-Cl-trityl–resin and peptide–Dbz–Rink–resin, while due to the



nature of the carbamate bond, is not permitted in the peptide-Dbz–Wang–resin.<sup>42</sup>

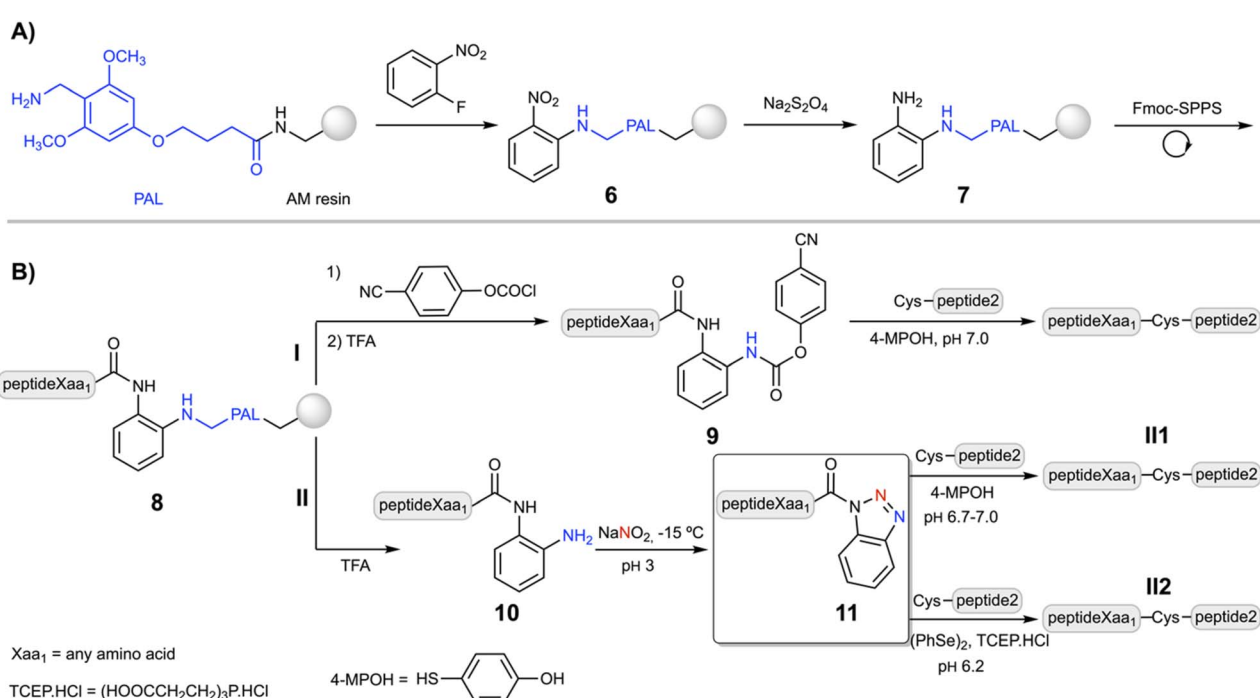
Then, we surmised that a labile aminomethyl-type linker could protect the Dbz from secondary acylations while still enabling the carbamoylation with chloroformate derivatives. The PAL linker is commercially available and widely used in Fmoc-SPPS.<sup>44</sup> Its acid lability is in between the 2-Cl-trityl and the Rink, and importantly, it can provide a similar selectivity like MeDbz–COOH, though sufficiently reactive towards chloroformates and alike compounds.

Following a similar synthetic route as for the synthesis of Fmoc–MeDbz–COOH,<sup>23</sup> 2-fluoronitrobenzene was added to the PAL–resin to give the (2-PAL)nitrobenzene–resin (**6**, Scheme 2A). The reduction of the nitro group of **6** was efficiently achieved in PEG and PEG-polystyrene resins using  $\text{Na}_2\text{S}_2\text{O}_4$  as a reducing agent under basic ( $\text{K}_2\text{CO}_3$ ) aqueous conditions (80–90%). However, due to the hydrophobic characteristics and low swelling properties of the polystyrene in  $\text{H}_2\text{O}$ , this route gave poor yields. The reduction was significantly improved in a DCM :  $\text{H}_2\text{O}$  (1 : 1) mixture using a transfer agent such as the tetrabutylammonium hydrogen sulfate, achieving conversions around 75% on the different types of polystyrene resins tested (see the ESI† for the resin manufacturers).<sup>45</sup>

The coupling of the first amino acid was accomplished in high yield (>99%) using HATU, although it is not strictly necessary for those amino acids with less bulky side chains. Fmoc-SPPS and chain elongation of **7** was carried out under standard conditions, using HBTU/DIEA or DIC/oxyma couplings (5 eq. of amino acid and the coupling agent),

without noticeable branching products, confirmed by the synthesis of the LYRAG<sub>5</sub>–Dbz peptide (Fig. S1†). Acylation of peptideXaa<sub>1</sub>–Dbz–PAL–resin (**8**, Xaa<sub>1</sub> = any amino acid, Scheme 2B) with *p*-nitrophenyl chloroformate followed by DIEA-induced cyclization gave the peptideXaa<sub>1</sub>–Nbz–PAL–resin peptide, confirmed by the yellow color of the *p*-nitrophenolate anion. Cleavage of the resin with TFA/scavengers (95%, v/v) yielded the expected peptideXaa<sub>1</sub>–Nbz product (LYRAF–Nbz, Fig. S2†). However, based on our own experience and the results of others in the preparation of C-terminal Nbz–CONH<sub>2</sub> and MeNbz–CONH<sub>2</sub> peptides (usually >30-mer), which can be slightly more problematic due to the intrinsic nature of the sequence,<sup>46</sup> we decided to adopt a more reliable strategy. This approach is based on the C-terminal (*p*CN–Phoc)MeDbz–CONH<sub>2</sub> peptides that undergo intramolecular cyclization to form the *N*-acylurea under aqueous conditions (Scheme 1 route A, conversion of **3** to **2**).<sup>24</sup>

Thus, after acylation of **8** with *p*-cyanophenyl chloroformate, the peptideXaa<sub>1</sub>–(*p*CN–Phoc)Dbz–PAL–resin (peptideXaa<sub>1</sub> = LYR(A/I)Xaa<sub>1</sub>; *p*CN–Phoc = *p*CN–phenyloxycarbonyl) was cleaved and simultaneously side chain deprotected using TFA/TIS/ $\text{H}_2\text{O}$  (95 : 2.5 : 2.5%, v/v) during two and a half hours to give the peptideXaa<sub>1</sub>–(*p*CN–Phoc)Dbz (**9**) in good yields (>85%) independently of the C-terminal amino acid, which indicates a wide scope of the method (92% for LYRAG–(*p*CN–Phoc)Dbz, Fig. S3†). Alternatively, cleavage of **8** (Scheme 2B route II) afforded the desired peptideXaa<sub>1</sub>–Dbz (**10**) in similar good overall yields (>90%) and crude purities, as shown for LYRAG–Dbz (95% crude recovery, Fig. S14†).



**Scheme 2** This work: (A) the 1,2-diaminobenzene–PAL strategy developed in this work for the synthesis of *o*-aminoanilide–PAL peptides. (B) Route I: synthesis of the peptideXaa<sub>1</sub>–(*p*CN–Phoc)Dbz and NCL. Route II: preparation of the peptideXaa<sub>1</sub>–Dbz precursor of the peptideXaa<sub>1</sub>–Bt and NCL mediated by peptideXaa<sub>1</sub>–(4-MPOH) thioesters (II1) and peptideXaa<sub>1</sub>–COSePh selenoesters (II2).



## Chemical ligations with peptideXaa<sub>1</sub>-(pCN-Phoc)Dbz and peptideXaa<sub>1</sub>-Dbz

**PeptideXaa<sub>1</sub>-(pCN-Phoc)Dbz.** Previously, we had shown that the peptideXaa<sub>1</sub>-(pCN-Phoc)MeDbz-CONH-G undergoes a slow cyclization to give the peptideXaa<sub>1</sub>-MeNbz-CONH-G at pH 7.4,<sup>24</sup> which is then trapped by 4-mercaptophenol (4-MPOH) yielding the peptideXaa<sub>1</sub>-(4-MPOH) thioester and the concomitant ligation in the presence of a Cys-peptide. When LYRAA-(pCN-Phoc)Dbz (**12**, 2 mM) was incubated in the presence of 4-MPOH (200 mM) and CRAFS (**13**, 3 mM, Fig. 1A), the expected ligation product LYRAACRAFS (**14**) was obtained, but a close inspection of the HPLC traces at different reaction times showed a singular reaction pathway (Fig. 1B). First, there is a quick exchange ( $t_{1/2} < 1$  min) of the *p*-cyanophenol moiety by 4-MPOH resulting in LYRAA-(pOH-phenylthiocarbonyl)Dbz (**15**, Fig. 1B and C). Following cyclization to give LYRAA-Nbz<sup>47</sup> (**16**, Fig. 1B and C), the concurrent thioesterification leads to LYRAA-(4-MPOH) (**17**, Fig. 1B and C) and the subsequent NCL. The reaction achieves a high conversion (98%) in under 3 h, and it is slower compared to that of LYRAA-Nbz/MeNbz-CONH-G (~1 h).<sup>22,23</sup> This difference in kinetics probably reflects major

stability of the Nbz due to a higher  $pK_a$  because of the lack of the CONH electron withdrawing group. A further confirmation of this result was supported by the relative stability at pH 7.0 of LYRAG-Nbz and LYRAG-Nbz-CONH-G. As expected, LYRAG-Nbz (70% intact peptide after 18 h) hydrolyzed at a slower rate than LYRAG-Nbz-CONH-G (50% intact peptide after 18 h, Fig. S40†). We next compared the reactivity of LYRAG-(pCN-Phoc)Dbz-CONH-G (**18**), LYRAG-(pCN-Phoc)MeDbz-CONH-G (**19**) and LYRAG-(pCN-Phoc)Dbz (**20**). The experiments were carried out in the presence of CLAFS (3 mM, 1.5 eq.) and 4-MPOH (200 mM) at pH 7 (Fig. 2A). The reactivity of the peptide **18** followed a similar reaction pathway to that of **20**: first, it undergoes a quick exchange with 4-MPOH to give LYRAG-(pOH-phenylthiocarbonyl)Dbz-CONH-G (<1 min), followed by a rapid cyclization and transthioesterification. The resulting LYRAG-(4-MPOH) is rapidly consumed in the ligation and almost did not accumulate. The slower transthioesterification kinetics of LYRAG-Nbz compared to LYRAG-Nbz-CONH-G determines the rate of the NCL, resulting in the fastest ligation for **18**. The longest reaction time corresponded to **19** as a consequence of the MeNbz formation being slowed down due to stereo-electronic effects of the methyl group, which also precluded the *O*-to-*S* exchange.

Fig. 2B and C show the product formation for the NCL between model peptides featuring different C-terminal amino acids (peptideXaa<sub>1</sub>-(pCN-Phoc)Dbz, 2 mM LYRAXaa<sub>1</sub>, Xaa<sub>1</sub> = G, A, F, H, Q, S, K, L, V and LYRIP-(pCN-Phoc)Dbz) and CXaa<sub>2</sub>AFS (3–3.5 mM; Xaa<sub>2</sub> = R, T, L), representative of model ligations displaying diverse kinetics, under aqueous conditions (6 M Gdm·HCl, 0.2 M NaPhos, 0.2 M 4-MPOH, 50 mM TCEP·HCl, pH = 6.8–7.0, and 22 °C). In all reactions, the conversion reached over 90% or close (88% for Pro) with only limited hydrolysis product as the major side product. Inspection of the kinetics showcased a sigmoidal plot-type behavior in which the ligated product started to form at around 5 min (Xaa<sub>1</sub> = G, A, F, Q, S, L, H at 1 min) or even later (V at 1 h and P at 3 h). All the intermediate species formed during the ligation of **12** (Fig. 1B and C) were also observed (Fig. S28–S38†). Cumulatively, the C-terminal amino acid does not have a strong influence in the *p*-cyanophenol-to-(4-MPOH) (**21**) exchange (<10 min, Fig. 2D). Then, the cyclization follows up to give the corresponding Nbz derivative (**22**) at a speed that, although it depends on Xaa<sub>1</sub>, is not rate limiting (Table S1†). Interestingly, in the absence of 4-MPOH, the cyclization in LYRAG-(pCN-Phoc)Dbz at pH 7.0 displayed a similar rate to LYRAG-(pOH-phenylthiocarbonyl) Dbz (Fig. S40†). However, we hypothesize that although it is conceivable that the formation of the *N*-acylurea (**22**) can occur through both species (**9** and **21**), the several-fold excess of 4-MPOH predominantly leads the cyclization *via* the thio-carbamate peptideXaa<sub>1</sub>-(pOH-phenylthiocarbonyl)Dbz derivative (**21**, Fig. 2D). Next, the peptideXaa<sub>1</sub>-Nbz (**22**) is intercepted by 4-MPOH yielding the thioester peptideXaa<sub>1</sub>-(4-MPOH) (**23**). This step is primarily rate limiting, as is clearly seen from the accumulation of LYRAV-Nbz and LYRIP-Nbz products during the reaction (Fig. 2C, S37 and S38†). Once the thioester is formed, it is ligated to yield the final peptideXaa<sub>1</sub>-CXaa<sub>2</sub>AFS (**24**). The slow transthioesterification step and the low effective

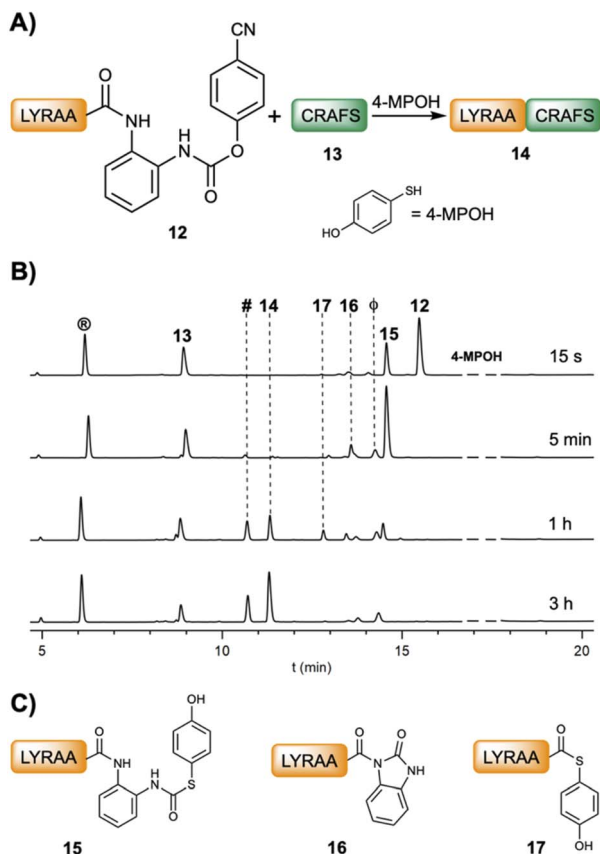


Fig. 1 (A) Scheme of the NCL between LYRAA-(pCN-Phoc)Dbz (**12**, 2 mM) and CRAFS (**13**, 3.0 mM) in 6 M Gdm·HCl, 0.2 M NaPhos, 0.2 M 4-MPOH, and 50 mM TCEP·HCl at pH 7.0. (B) HPLC traces at 220 nm of the ligation at different times.  $\textcircled{R}$  = L-Tyr,  $\#$  = 2-benzimidazolinone (Nbz);  $\phi$  = *p*-cyanophenol. (C) Chemical structures of the intermediates LYRAA-(pOH-phenylthiocarbonyl)Dbz (**15**), LYRAA-Nbz (**16**) and LYRAA-(4-MPOH) (**17**).



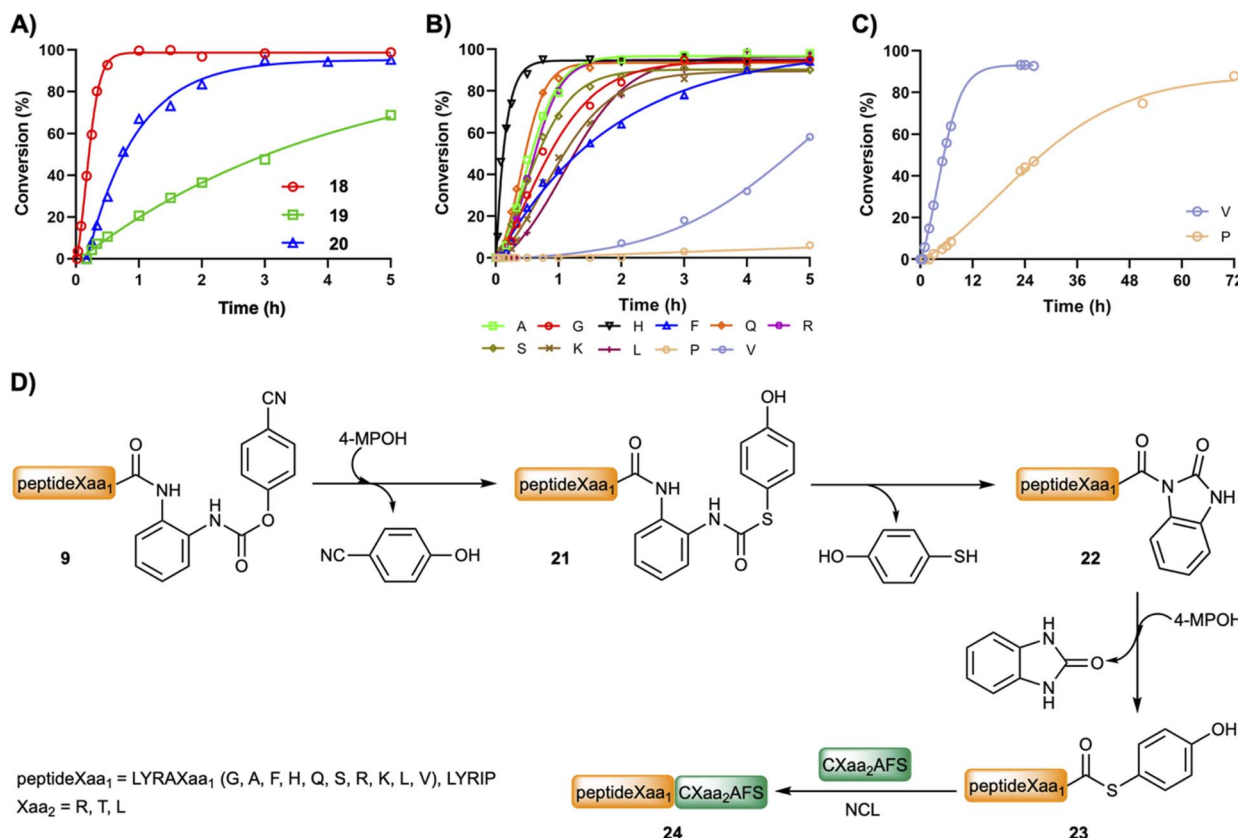


Fig. 2 (A) Kinetics of the ligation between CLAFS and LYRAG-(pCN-Phoc)Dbz-CONH-G (18) and LYRAG-(pCN-Phoc)MeDbz-CONH-G (19) and LYRAG-(pCN-Phoc)Dbz (20). (B) Plot of the fraction ligated of LYRAXaa<sub>1</sub>CXaa<sub>2</sub>AFS. (C) Formation of LYRAVCTAFS and LYRIPCTAFS. (D) Plausible mechanism for the ligation. Reactions were carried out at pH 6.8–7.0 in 6 M Gdm·HCl and 0.2 M NaPhos at 22 °C. Concentrations of the peptides were: [LYRAXaa<sub>1</sub>-(pCN-Phoc)Dbz, LYRIP-(pCN-Phoc)Dbz] = 2 mM; [CXaa<sub>2</sub>AFS] = 3–3.5 mM.

concentration of LYRAV-(4-MPOH) and LYRIP-(4-MPOH) explain the longer reaction times, particularly significant in the case of LYRIP-(4-MPOH) (72 h), since this ligation achieves similar conversions in 20 h when the concentration of LYRIP-(4-MPOH) is in the millimolar range (Table 1).

Table 1 Conversions for the two-step one-pot ligations between CXaa<sub>2</sub>AFS (Xaa<sub>2</sub> = R, T, L) and the model peptides LYRAXaa<sub>1</sub>-Dbz and LYRIP-Dbz displaying different C-terminal Xaa<sub>1</sub> amino acids<sup>a</sup>

Entry	C-Terminal Xaa <sub>1</sub>	Time (h)	Conversion (%)
1	G	0.5	93
2	A	1	99
3	F	1	90
4	H	0.5	92
5	Q	1	85
6	K	1	95
7	R	1	91
8	S	1	94
9	L	1	88
10	V	8	86
11	P	20	84

<sup>a</sup> NCL was carried out at pH 6.7–7.0 in 6 M Gdm·HCl and 0.2 M NaPhos at 22 °C. Concentrations of the peptides were: [LYRAXaa<sub>1</sub>-Dbz, LYRIP-Dbz] = 2.2–2.5 mM; [CXaa<sub>2</sub>AFS] = 4.3–4.7 mM.

Finally, thioesterification in solution using the peptideXaa<sub>1</sub>-(pCN-Phoc)Dbz appears to be a better strategy for the preparation of peptideXaa<sub>1</sub>-COSR because it prevents the formation of the peptide-Nbz on resin followed by the cleavage, which seems slightly problematic in the preparation of some peptide-Nbz/MeNbz-CONH-G derivatives.<sup>46</sup>

**PeptideXaa<sub>1</sub>-Dbz.** The reactivity of peptideXaa<sub>1</sub>-Dbz (10, Scheme 2B route II) is different from that of the peptideXaa<sub>1</sub>-(pCN-Phoc)Dbz (9, Scheme 2B route I): first, in order to activate the peptide, the addition of NaNO<sub>2</sub> (3.5 eq.) at acidic pH 3 and low temperature (~−15 °C) is necessary. These conditions preserve the selectivity by preventing the potential oxidation of other sensitive functional groups present in Met, Cys, Tyr, Trp, Lys or the N-terminal amine. Second, the transthioesterification of peptideXaa<sub>1</sub>-Bt (11) has a low energy barrier, and the *N*-to-*S* acyl transfer is not rate limiting (<5 min for all Xaa<sub>1</sub> tested), contrarily to the peptideXaa<sub>1</sub>-Nbz (22), rendering the peptideXaa<sub>1</sub>-COSR at pH 5–7 and 0 °C in the presence of the corresponding thiol (200 mM, Scheme 2B route II1). The thioesterification is not strongly dependent on the C-terminal amino acid, since it is equally rapid when the C-terminal amino acid is Pro (Fig. S52†).

The ligation could be carried out stepwise (Fig. 3) or in a two-step one-pot fashion (Table 1). For instance, in a stepwise

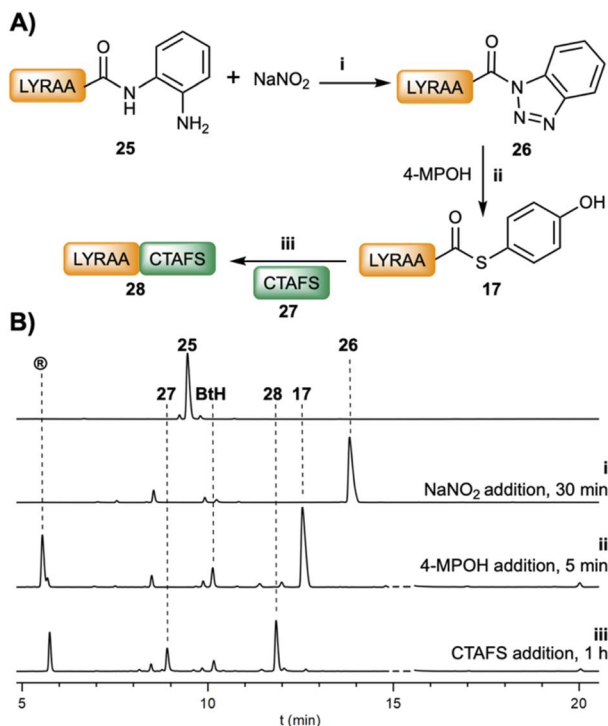


Fig. 3 (A) Scheme of the stepwise ligation between LYRAA-Dbz (25, 2.5 mM) and CTAFS (27, 4.7 mM): (i) NaNO<sub>2</sub> (3.5 eq.) oxidation at  $-15^{\circ}\text{C}$ , pH = 3, and 30 min; (ii) addition of 4-MPOH (200 mM) and TCEP·HCl (50 mM) at pH = 6.7; (iii) NCL, addition of CTAFS (27). (B) HPLC traces at 220 nm of the reaction after (i) (NaNO<sub>2</sub> addition), (ii) (4-MPOH addition) and (iii) (CTAFS addition) steps. – = 4-MPOH.

manner, after the oxidation of LYRAA-Dbz (25, 30 min, Fig. 3) to afford LYRAA-Bt (26), the reaction is diluted in a larger volume of a 4-MPOH solution, which also quenches the excess of NaNO<sub>2</sub>, and the pH is adjusted to 6.7–7.0. Remarkably, the LYRAA-Bt fragment can be characterized by HPLC and mass spectrometry (MALDI-TOF). Then, CTAFS (27) is added to the resulting LYRAA-(4-MPOH) (17) to initiate the ligation, which is complete in under 1 h.

Studies on the stability of LYRAG-Bt and LYRAG-Bt-CONH-G at pH 7 (Fig. S53†) revealed a higher stability of the former ( $t_{1/2} \approx 16$  min, 28% remaining peptide after 0.5 h vs. ~2%), although much lower compared to LYRAG-Nbz (Fig. S40†). Nevertheless, bearing in mind that the transacylation reaction occurs on the time scale of seconds, we consider that the Bt approach is superior to the Bt-CONH-G strategy for the preparation of peptide-COSR. Indeed, the direct ligation of LYRIP-Bt and CTAFS gave an interesting 33% of the ligated LYR-IPCTAFS peptide (Fig. S54†).<sup>48</sup>

When the reaction is performed in one pot (Table 1), the peptideXaa<sub>1</sub>-Dbz (2.2–2.5 mM) and CXaa<sub>2</sub>AFS (4.3–4.7 mM) were dissolved in buffer (6 M Gdm·HCl, 0.2 M NaPhos, pH = 3.0,  $\sim -15^{\circ}\text{C}$ ). Then, NaNO<sub>2</sub> (3.5 eq. pertaining to peptideXaa<sub>1</sub>-Dbz) was added, and the oxidation was carried out for 30 min. Of note, in the case of Xaa<sub>1</sub> = P, for the Bt formation, it was necessary to leave it at 0 °C to achieve complete conversion. Following up, the reaction was diluted in a larger volume of 4-

MPOH buffer (200 mM; final pH of the ligation is around 6.7–7.0) that started the ligation. It is noticeable that, under these ligation conditions, the N-terminal cysteine was not modified due to either the low pH of the oxidation or because the 4-MPOH can revert the S-nitrosylation of the β-mercaptop group.<sup>14</sup> The conversions achieved were over 90% for almost all peptides (except when Xaa<sub>1</sub> = Q, L, V, P), and significantly faster than the Nbz-mediated ligation: 1 h for all peptides tested, except when Xaa<sub>1</sub> was V (8 h) and P (20 h).

We have noticed that, although the Bt approach is compatible with stepwise or two-step one-pot reactions, in our experience, the chemical ligation of large peptide-COSR fragments (>20-mer) is more reliable by using a stepwise methodology. Thus, it is recommended that the peptide-Bt is first converted into a more stable peptide-COSR (R = alkyl) such as peptide-MESNa (MESNa = 2-mercaptopethanesulfonic acid sodium salt) and then ligated.

**PeptideXaa<sub>1</sub>-COSePh.** Peptide selenoesters (peptide-COSeR) have attracted a lot of attention in recent years. In a seminal study, a peptide-COSeR featuring an intractable C-terminal slow-reacting Pro showed an increase of one order of magnitude in the NCL rate.<sup>8</sup> The superior acylation capacity of the peptide-COSeR is the basis for the newly developed diselenide-selenoester ligation wherein the peptide-COSeR reacts in the presence of an N-terminal diselenide peptide to afford the ligation of both peptides.<sup>9</sup> Despite the potential of this ligation, the synthesis of the peptide-COSeR has remained elusive. The use of protected peptides has limitations due to the potential racemization of the C-terminal amino acid and the low solubility of the protected fragments.

Recently, an approach based on unprotected C-terminal peptide pyrazoles prepared from peptide hydrazides yielded the corresponding peptide-COSeR,<sup>49</sup> a methodology that has been further applied to a novel expressed protein-COSeR ligation.<sup>50</sup> Accordingly, the synthesis of C-terminal peptide-COSeR would be greatly benefited by general methods that, starting from readily available selenoester precursors, facilitate an efficient conversion under smooth conditions. Following this premise, we investigated if the peptideXaa<sub>1</sub>-Nbz or the peptideXaa<sub>1</sub>-Bt could undergo acyl exchange in the presence of benzeneselenol. Thus PhSeH, generated *in situ* from the reduction of diphenyldiselenide (50 mM) using TCEP (100 mM), was incubated in the presence of LYRAF-Nbz (2 mM). However, only trace amounts of LYRAF-COSePh were detected after 2 h of reaction, confirming the previous results.<sup>8</sup> In sharp contrast, LYRAF-Bt readily exchanged to give LYRAF-COSePh (<1 min, 30, Fig. 4B). This result was not surprising and reassures the superior acyl transfer characteristics of the Bt group. Stepwise NCL of LYRAF-Dbz (29, 2.2 mM, Fig. 4A), activated with NaNO<sub>2</sub> (3.5 eq.), and CTAFS (27, 4.7 mM) yielded the ligated LYRAF-CTAFS (32) product in 15 min (95% conversion). Very interestingly, under these NCL conditions (pH 6.0–6.2), a product (31) with a shorter HPLC retention time that had a mass identical to the ligated peptide (32), was detected during the first seconds of the reaction. We tentatively hypothesize and assign this compound to the *S*-acyl LYRAF(S)CTAFS (Fig. S55†) intermediate formed by the transacylation of LYRAF-COSePh (30)

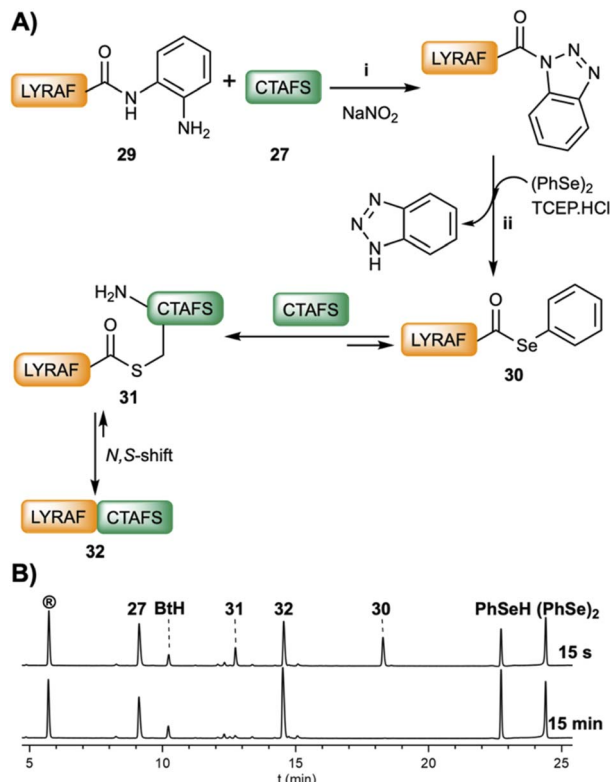


**Fig. 4** (A) Scheme of the stepwise ligation between LYRAF-Dbz (29, 2.2 mM) and CTAFS (27, 4.7 mM): (i)  $\text{NaNO}_2$  (3.5 eq.) oxidation at  $-15^\circ\text{C}$ ; pH = 3, 30 min; (ii) addition of  $(\text{PhSe})_2$  (50 mM) and TCEP·HCl (100 mM) at pH = 6.2. (B) HPLC traces at 220 nm of the reaction after addition of  $(\text{PhSe})_2$  and TCEP·HCl at 15 s and 15 min.

and CTAFS (27). Studies to determine the correct structure of this intermediate are underway.

The fast and clean selenoester conversion imparted to the peptide-Bt intermediates is a very promising approach for selenoester-based ligations, especially at those sites in which the kinetics of the reaction is prohibitively slow or the concentration of the reaction partners is in the micromolar range.

### Synthesis of the glucocorticoid receptor DNA binding domain

The glucocorticoid receptor (GR) is a transcription factor (TF) belonging to the zinc finger family. The GR is involved in the inflammatory response and cell growth, proliferation and survival.<sup>51</sup> The DNA binding domain of the GR (GR DBD) spans a region of about 75 amino acids (418–493) and contains two zinc atoms tetracoordinate by four Cys residues, each Zn atom adopting a tetrahedral conformation (Fig. 5A and B). The GR proteins bind the GRE response elements (AGAACAAaaTGTTCT) as homodimers (Fig. 5A), activating or repressing the transcription of the target genes depending on the cell state.<sup>52–54</sup> The GR has been and continue to be an important target for drug development.

For the CPS of the GR DBD (amino acids from 419 to 495), a linear synthesis comprising three fragments (Fig. 5B and C) was designed: F1 (419–437), F2 (438–475) and F3 (476–495). F1 and F2 were assembled on a ChemMatrix resin (Fig. S56 and

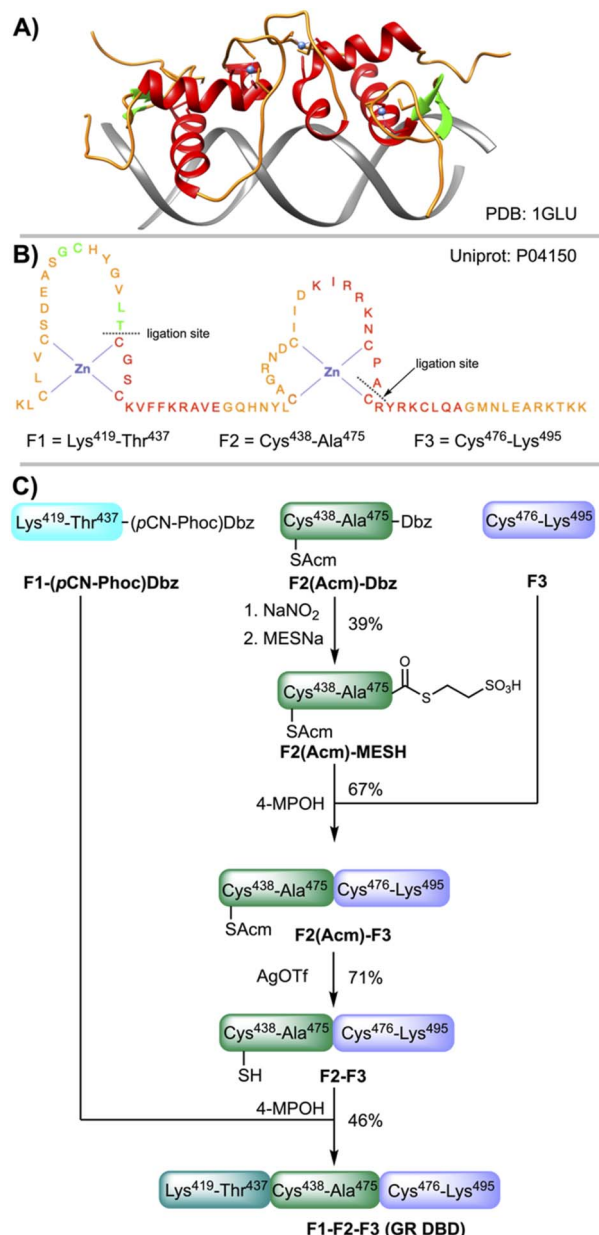


**Fig. 5** (A) X-Ray structure of the homodimer DNA binding domain (DBD) of the glucocorticoid receptor (GR) bound to the GRE site (AGAACAAaaTGTTCT).<sup>53</sup> The red color denotes the  $\alpha$ -helix, green the  $\beta$ -strand, orange the interconnecting loops and blue the Zn atoms. (B) Sequence of the Zn finger domain of the human GR and fragments F1, F2 and F3 used for CPS. (C) Synthetic scheme of the GR assembled linearly from three fragments: first F2 + F3; second F1 + F2-F3.

S57†) and F3 in a 2-Cl-trityl functionalized resin (Fig. S58†). For F1 and F2, following the coupling of PAL and 2-fluoroni-trobenzene, the nitro group was reduced to give the corresponding Dbz-PAL-resin. After chain elongation, F1 was acylated with *p*-cyanophenyl chloroformate. Next, the peptide F1-(pCN-Phoc)Dbz was cleaved from the resin and isolated in a good crude purity ( $\sim$ 60% by analytical HPLC) and recovery yield (70%). F2(Acm)-Dbz was prepared following a similar strategy ( $\sim$ 70% crude purity, 70% recovery yield), using the Acm

instead of the thiazolidine protection for the sulphydryl of the N-terminal Cys in order to prevent the nitrosylation of the  $\alpha$ -amino group.

For the ligation of F2(Acm) and F3, although it could be carried out in a two-step one-pot approach, we found that the conversion to F2(Acm)-MESH enables a more reliable and scalable synthesis. Thus, F2(Acm)-Dbz was first transformed into the more stable F2(Acm)-MESH thioester (39% based on the F2(Acm)-Dbz crude) and then assembled with F3 in a good

yield (67%, Fig. 5C, 6A(i and ii)). Remarkably, it is important to point out that despite the presence of the multiple Cys residues in the fragment F2, none of these were nitrosylated under the reaction conditions: (i) 10 eq. NaNO<sub>2</sub>, pH 3, and  $-15\text{ }^\circ\text{C}$  and (ii) 100 mM MESNa, highlighting the exclusive chemospecificity of the oxidation-thioesterification process.

Following the condensation of F2(Acm) and F3, the Acm group was removed under standard conditions (50 mM AgOTf in H<sub>2</sub>O : AcOH, Fig. 6A(iii), 71%). Next, F1-(*p*CN-Phoc)Dbz was ligated to F2-F3 to achieve the synthesis of the linear sequence (46%, Fig. 6A(iv-vi)). A closer inspection of the final ligation after 2 h of reaction (Fig. 6A(v)) revealed all the intermediates resulting from the mechanism depicted above (Fig. 2D), including also the possible cyclic thiolactones formed by the intramolecular attack of the internal Cys of F1 to the C-terminal Thr. The ESIMS corroborated the expected linear F1-F2-F3 GR Zn finger domain (Lys<sup>419</sup>-Lys<sup>495</sup>, Fig. 6B).

Zn finger domains adopt a particular folding upon incubation with Zn<sup>2+</sup>, represented by the prototypical TFIIIA from *Xenopus*.<sup>55,56</sup> The metal in the Zn finger of TFIIIA is tetra-coordinated by two Cys and two His residues. In the GR DBD, the metal also adopts a tetrahedral sphere, but instead it is coordinated by four Cys residues that fold the resulting structure in a different conformation. This configuration displays a particular circular dichroism signature that mainly reflects the contribution of the predominant  $\alpha$ -helical motifs. When the synthetic GR DBD linear peptide (35  $\mu\text{M}$ ) was incubated in the presence of increasing concentrations of ZnCl<sub>2</sub> (0–40  $\mu\text{M}$ ), an increase in the band at 222 nm was observed, while at 208 nm, it decreased, indicative of the formation of an  $\alpha$ -helix induced by the nucleation of the Zn atom (Fig. 6C). Electrophoretic mobility shift assays in non-denaturing polyacrylamide-bisacrylamide gels showed a complex between the GR DBD and the GRE cognate sequence (Fig. 6D). In addition, MALDI-TOF mass spectrometry showed the Zn finger folded structure by the detection of the [M + Zn]<sup>+</sup> and [M + 2Zn]<sup>+</sup> ions (Fig. S64†).

## Conclusions

In summary, here we have presented the Dbz, a simplified version of the *o*-aminoanilide moieties for CPS. Coupled with the PAL linker, it leverages the monoacylation selectivity imparted by the MeDbz-COOH and delivers *o*-aminoanilide peptides that can be cleaved directly from the resin to give the peptide-Dbz or first carbamoylated and then cleaved to afford the peptide-(aryloxy carbonyl)Dbz. The resulting activated peptide-Nbz and peptide-Bt are more stable than the corresponding peptide-Nbz/MeNbz-CONH-G and peptide-Bt-CONH-G but also labile enough to undergo thiolysis. In particular, the peptide-Bt is more functional and provides fast (<5 min) and scalable (mg quantities) peptide-COSR products. Very remarkably, the superior acylating properties of the peptide-Bt over the peptide-Nbz also permit the selenoesterification in the presence of benzeneselenol at a similar rate to that of the thioesterification. Selenoesters have found a wide range of applications in the recent years including faster kinetics at sterically demanding residues and diselenide-

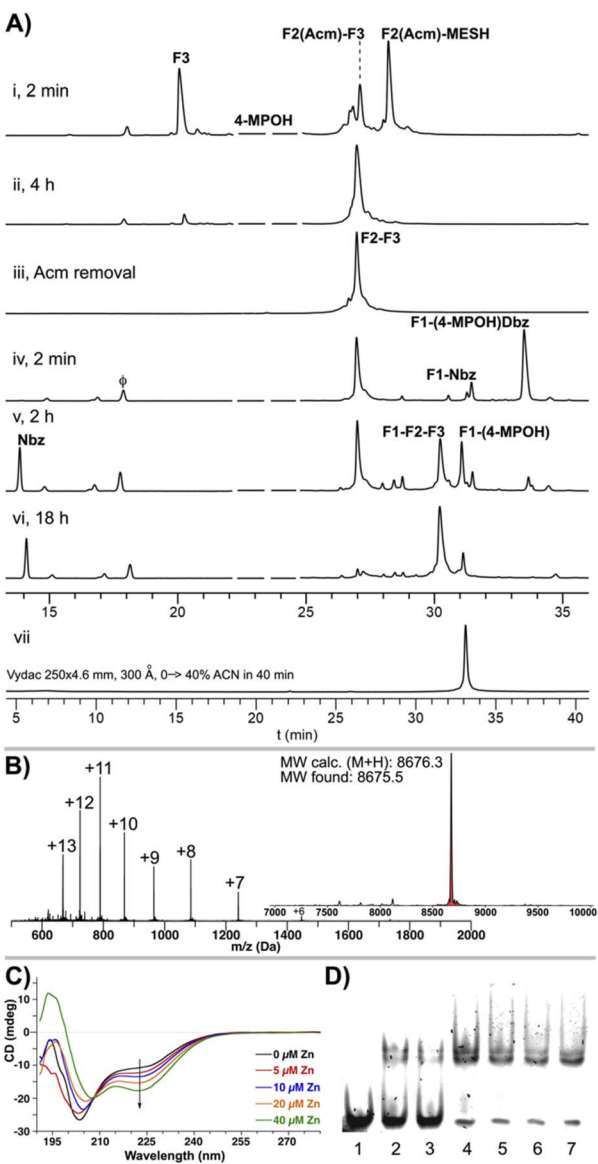


Fig. 6 (A) HPLC traces at 220 nm of the CPS of the GR DBD: (i) F2(Acm)-MESH + F3 at 2 min and (ii) at 4 h, (iii) Acm removal from F2(Acm)-F3, (iv) F1-(*p*CN-Phoc)Dbz + F2-F3 at 2 min, (v) 2 h and (vi) 6 h, (vii) analytical HPLC trace at 220 nm of a purified sample of F1-F2-F3. ACN = acetonitrile.  $\phi$  = *p*-cyanophenol. (B) ESIMS of F1-F2-F3 (Lys<sup>419</sup>-Lys<sup>495</sup>) and the deconvoluted mass spectrum. (C) Circular dichroism spectra of the GR DBD (35  $\mu\text{M}$ ) in the presence of increasing concentrations of ZnCl<sub>2</sub>: 0, 5, 10, 20, and 40  $\mu\text{M}$ . (D) Electrophoretic mobility shift assay of the GR DBD and GRE. [GR DBD] lanes 1–7 = 0, 0.6, 0.8, 1.0, 1.4, 1.8, and 2.3  $\mu\text{M}$ .



selenoester ligations. We foresee that the Dbz approach will find wide application within all the selenoester-based technologies for peptide ligations.

## Data availability

All experimental data and detailed experimental procedures are available in the ESI,† and from the corresponding author upon request.

## Author contributions

I. S.-C.: conceptualization, investigation, formal analysis, methodology, visualization and writing. J. M.-G.: investigation and formal analysis. P. K.: investigation and formal analysis. J. B. B.-C.: conceptualization, investigation, methodology, visualization, funding acquisition, supervision and writing. All authors have read, commented and given approval to the final version of the manuscript.

## Conflicts of interest

The authors declare that there are no conflicts of interest.

## Acknowledgements

This work has received funding from the grants RTI2018-096323-I00, PDI2021-128902OB-I00 (Spanish Ministerio de Ciencia e Innovación) and LCF/PR/HR20/52400006 ('la Caixa' Foundation). I. S.-C. thanks the AGAUR (Generalitat of Catalonia) for a predoctoral fellowship (2021 FI-B 00142), and P. K. thanks the Erasmus+ programme (European Commission) for a mobility fellowship. Rosaria Ragozzino (Erasmus+, University of Naples) is acknowledged for the preliminary electrophoretic experiments.

## Notes and references

- 1 P. E. Dawson, T. W. Muir, I. Clark-Lewis and S. B. H. Kent, *Science*, 1994, **266**, 776.
- 2 P. E. Dawson and S. B. H. Kent, *Annu. Rev. Biochem.*, 2000, **69**, 923.
- 3 T. W. Muir, D. Sondhi and P. A. Cole, *Proc. Natl. Acad. Sci. U. S. A.*, 1998, **95**, 6705.
- 4 L. E. Canne, S. J. Bark and S. B. H. Kent, *J. Am. Chem. Soc.*, 1996, **118**, 5891.
- 5 J. Offer, C. N. C. Boddy and P. E. Dawson, *J. Am. Chem. Soc.*, 2002, **124**, 4642.
- 6 A. C. Conibear, E. E. Watson, R. J. Payne and C. F. W. Becker, *Chem. Soc. Rev.*, 2018, **47**, 9046, and references cited therein.
- 7 O. Fuchs, S. Trunschke, H. Hanebrink, M. Reimann and O. Seitz, *Angew. Chem., Int. Ed.*, 2021, **60**, 19483.
- 8 T. Durek and P. F. Alewood, *Angew. Chem., Int. Ed.*, 2011, **50**, 12042.
- 9 N. J. Mitchell, L. R. Malins, X. Liu, R. E. Thompson, B. Chan, L. Radom and R. J. Payne, *J. Am. Chem. Soc.*, 2015, **137**, 14011.
- 10 Y. Shin, K. A. Winans, B. J. Backes, S. B. H. Kent, J. A. Ellman and C. R. Bertozzi, *J. Am. Chem. Soc.*, 1999, **121**, 11684.
- 11 R. Ingenito, E. Bianchi, D. Fattori and A. Pessi, *J. Am. Chem. Soc.*, 1999, **121**, 11369.
- 12 A. P. Tofteng, K. K. Sørensen, K. W. Conde-Frieboes, T. Hoeg-Jensen and K. J. Jensen, *Angew. Chem., Int. Ed.*, 2009, **48**, 7411.
- 13 H. E. Elashal, Y. E. Sim and M. Raj, *Chem. Sci.*, 2017, **8**, 117.
- 14 G.-M. Fang, Y.-M. Li, F. Shen, Y.-C. Huang, J.-B. Li, Y. Lin, H.-K. Cui and L. Liu, *Angew. Chem., Int. Ed.*, 2011, **50**, 7645.
- 15 N. Ollivier, J. Dheur, R. Mhidia, A. Blannpain and O. Melnyk, *Org. Lett.*, 2010, **12**, 5238.
- 16 P. Botti, M. Villain, S. Manganiello and H. Gaertner, *Org. Lett.*, 2004, **26**, 4681.
- 17 J. D. Warren, J. S. Miller, S. J. Keding and S. J. Danishefsky, *J. Am. Chem. Soc.*, 2004, **126**, 6576.
- 18 K. Sato, A. Shigenaga, K. Tsuji, S. Tsuda, Y. Sumikawa, K. Sakamoto, A. Otaka, K. Sato, A. Shigenaga, K. Tsuji, S. Tsuda, Y. Sumikawa, K. Sakamoto and A. Otaka, *ChemBioChem*, 2011, **12**, 1840.
- 19 J.-S. Zheng, H.-N. Chang, F.-L. Wang and L. Liu, *J. Am. Chem. Soc.*, 2011, **133**, 11080.
- 20 J.-X. Wang, G.-M. Fang, Y. He, D.-L. Qu, M. Yu, Z.-Y. Hong and L. Liu, *Angew. Chem., Int. Ed.*, 2015, **54**, 2194.
- 21 J. Weidmann, E. Dimitrijević, J. D. Hoheisel and P. E. Dawson, *Org. Lett.*, 2016, **18**, 164.
- 22 J. B. Blanco-Canosa and P. E. Dawson, *Angew. Chem., Int. Ed.*, 2008, **47**, 6851.
- 23 J. B. Blanco-Canosa, B. Nardone, F. Albericio and P. E. Dawson, *J. Am. Chem. Soc.*, 2015, **137**, 7197.
- 24 J. Palà-Pujadas, F. Albericio and J. B. Blanco-Canosa, *Angew. Chem., Int. Ed.*, 2018, **57**, 16120.
- 25 D. T. Flood, J. J. Hintzen, M. J. Bird, P. A. Cistrone, J. Ason, S. Chen and P. E. Dawson, *Angew. Chem., Int. Ed.*, 2018, **57**, 11634.
- 26 S. K. Mahto, C. J. Howard, J. C. Shimko and J. J. Ottesen, *ChemBioChem*, 2011, **12**, 2488.
- 27 J. Mannuthodikayil, S. Singh, A. Biswas, A. Kar, W. Tabassum, P. Vydyam, M. K. Bhattacharyya and K. Mandal, *Org. Lett.*, 2019, **21**, 9040.
- 28 K. S. A. Kumar, L. Spasser, L. A. Erlich, S. N. Bavikar and A. Brik, *Angew. Chem., Int. Ed.*, 2010, **48**, 9126.
- 29 S. Gunasekera, T. L. Aboye, W. A. Madian, H. R. El-Seedi and U. Göransson, *Int. J. Pept. Res. Ther.*, 2013, **19**, 43.
- 30 B. Fauvet, S. M. Butterfield, J. Fuks, A. Brik and H. A. Lashuel, *Chem. Commun.*, 2013, **49**, 9254.
- 31 L. Dery, P. S. Reddy, R. Mousa, O. Ktorza, A. Talhami and N. Metanis, *Chem. Sci.*, 2017, **8**, 1922.
- 32 Z. Zhao, R. Mousa and N. Metanis, *Chem.-Eur. J.*, 2022, **28**, e202200279.
- 33 A. Baral, A. Asokan, V. Bauer, B. Kieffer and V. Torbeev, *Tetrahedron*, 2019, **75**, 703.
- 34 A. R. Katritzky, A. A. Shestopalov and K. Suzuki, *Synthesis*, 2004, **2004**, 1806.
- 35 D. Bang, B. L. Pentelute and S. B. H. Kent, *Angew. Chem., Int. Ed.*, 2006, **45**, 3985.



36 C. A. Arbour, T. D. Kondasinghe, H. Y. Saraha, T. L. Vorlicek and J. L. Stockdill, *Chem. Sci.*, 2018, **9**, 350.

37 C. A. Arbour, R. E. Stamatin and J. L. Stockdill, *J. Org. Chem.*, 2018, **83**, 1797.

38 C. A. Arbour, L. G. Mendoza and J. L. Stockdill, *Org. Biomol. Chem.*, 2020, **18**, 7253.

39 A. Selvaraj, H.-T. Chen, A. Y.-T. Huang and C.-L. Kao, *Chem. Sci.*, 2018, **9**, 345.

40 T. Ohara, M. Kaneda, T. Saito, N. Fujii, H. Ohno and S. Oishi, *Bioorg. Med. Chem. Lett.*, 2018, **28**, 1283.

41 G. A. Acosta, L. Murray, M. Royo, B. G. de la Torre and F. Albericio, *Front. Chem.*, 2020, **8**, 298.

42 J. Weidmann, M. Schnölzer, P. E. Dawson and J. D. Hoheisel, *Cell Chem. Biol.*, 2019, **26**, 645.

43 F. J. Ferrer-Gago and L. Q. Koh, *Pept. Sci.*, 2021, **113**, e24194.

44 F. Albericio and G. Barany, *Int. J. Pept. Protein Res.*, 1987, **30**, 206.

45 R. Kaplánek and V. Krchnák, *Tetrahedron Lett.*, 2013, **54**, 2600.

46 P. W. R. Harris and M. A. Brimble, *Biopolymers*, 2013, **100**, 356.

47 The Nbz was first described by Pascal as a carboxyl-protecting and activating group in peptides: R. Pascal, D. Chauvey and R. Sola, *Tetrahedron Lett.*, 1994, **35**, 6291.

48 Some peptideXaa<sub>1</sub>-Bt (Xaa<sub>1</sub> = V, P) derivatives could be isolated by HPLC purification, although they slowly hydrolyze in the form of lyophilized powders.

49 Y. Li, J. Liu, Q. Zhou, J. Zhao and P. Wang, *Chin. J. Chem.*, 2021, **39**, 1861.

50 S. S. Kulkarni, E. E. Watson, J. W. C. Maxwell, G. Niederacher, J. Johansen-Leete, S. Huhmann, S. Mukherjee, A. R. Norman, J. Kriegesmann, C. F. W. Becker and R. J. Payne, *Angew. Chem., Int. Ed.*, 2022, **61**, e202200163.

51 E. R. Weikum, M. T. Knuesel, E. A. Ortlund and K. R. Yamamoto, *Nat. Rev. Mol. Cell Biol.*, 2017, **18**, 159.

52 V. L. Chandler, B. A. Maler and K. R. Yamamoto, *Cell*, 1983, **33**, 489.

53 B. F. Luisi, W. X. Xu, Z. Otwinowski, L. P. Freedman, K. R. Yamamoto and P. B. Sigler, *Nature*, 1991, **352**, 497.

54 S. H. Meijsing, M. A. Pufall, A. Y. So, D. L. Bates, L. Chen and K. R. Yamamoto, *Science*, 2009, **324**, 407.

55 J. Miller, A. D. McLachlan and A. Klug, *EMBO J.*, 1985, **4**, 1609.

56 R. S. Brown, C. Sander and P. Argos, *FEBS Lett.*, 1985, **186**, 274.

